Published in final edited form as:
J Autoimmun. 2011 August ; 37(1): 48–57. doi:10.1016/j.jaut.2011.03.004.

The SLAM family member CD48 (*Slamf2*) protects lupus-prone mice from autoimmune nephritis

Anna E. Koh[a,b], **Sarah W. Njoroge**[a,b], **Marianela Feliu**[a,b], **Alexis Cook**[b], **Martin K. Selig**[c], **Yvette E. Latchman**[d,e], **Arlene H. Sharpe**[d], **Robert B. Colvin**[c], and **Elahna Paul**[b]

Anna E. Koh: aekoh417@gmail.com; Sarah W. Njoroge: sarah.w.njoroge@vanderbilt.edu; Marianela Feliu: feliu20m@mtholyoke.edu; Alexis Cook: acook3@partners.org; Martin K. Selig: mselig@partners.org; Yvette E. Latchman: yvettel@psbcresearch.org; Arlene H. Sharpe: arlene_sharpe@hms.harvard.edu; Robert B. Colvin: colvin@helix.mgh.harvard.edu

[b]Division of Pediatric Nephrology, Harvard Medical School and Massachusetts General Hospital, 55 Fruit St., Boston, MA 02114

[c]Department of Pathology, Harvard Medical School and Massachusetts General Hospital, 55 Fruit St., Boston, MA 02114

[d]Departments of Pathology, Harvard Medical School and Brigham and Women's Hospital, 77 Avenue Louis Pasteur, Boston, MA 02115

Abstract

Polymorphisms in the SLAM family of leukocyte cell surface regulatory molecules have been associated with lupus-like phenotypes in both humans and mice. The murine *Slamf* gene cluster lies within the lupus-associated *Sle1b* region of mouse chromosome 1. Non-autoreactive C57BL/6 (B6) mice that have had this region replaced by syntenic segments from other mouse strains (*i.e.* 129, NZB and NZW) are B6 congenic strains that spontaneously produce non-nephritogenic lupus-like autoantibodies. We have recently reported that genetic ablation of the SLAM family member CD48 (*Slamf2*) drives full-blown autoimmune disease with severe proliferative glomerulonephritis (CD48GN) in B6 mice carrying 129 sequences of the *Sle1b* region (B6.129CD48$^{-/-}$). We also discovered that BALB/c mice with the same 129-derived CD48-null allele (BALB.129CD48$^{-/-}$) have neither nephritis nor anti-DNA autoantibodies, indicating that strain specific background genes modulate the effects of CD48 deficiency. Here we further examine this novel model of lupus nephritis in which CD48 deficiency transforms benign autoreactivity into fatal nephritis. CD48GN is characterized by glomerular hypertrophy with mesangial expansion, proliferation and leukocytic infiltration. Immune complexes deposit in mesangium and in sub-endothelial, sub-epithelial and intramembranous sites along the glomerular basement membrane. Afflicted mice have low grade proteinuria, intermittent hematuria and their progressive renal injury manifests with elevated urine NGAL levels and with uremia. In contrast to the lupus-like B6.129CD48$^{-/-}$ animals, neither BALB.129CD48$^{-/-}$ mice nor B6 × BALB/c F1.129CD48$^{-/-}$ progeny have autoimmune traits, indicating that B6-specific background genes modulate the effect of CD48 on lupus nephritis in a recessive manner.

Corresponding author: Elahna Paul, MD, PhD, MGH Pediatric Nephrology YAW-6C, 55 Fruit St., Boston, MA 02114, tel: 617-724-2896, fax: 617-724-3248, epaul@partners.org.
[a]These authors contributed equally to this work.
[e]Present address: Puget Sound Blood Center, 921 Terry Avenue, BRI 3015, Seattle, WA 98104

Keywords

CD48(*Slamf2*); lupus nephritis; anti-DNA autoantibodies; systemic lupus erythematosus; murine lupus; *Sle1b*

1. Introduction

Overt glomerulonephritis (GN) occurs in up to two-thirds of patients with systemic lupus erythematosus (SLE), while silent GN is estimated to exist in many, if not most, of the remaining individuals affected by this disease. Multiple genes contribute to the autoimmune manifestations of SLE in numerous mouse models as well as in human populations. Insight into epistatic gene effects on the progression and severity of lupus is in its infancy, growing with successive discoveries of novel disease modifiers and genetic interactions in multiple model systems.

Members of the SLAM family of cell surface proteins have been implicated as immunomodulators in tolerance and autoimmune disease. Polymorphisms within this gene family have been associated with lupus-like phenotypes in both humans and mice [1-3]. Genes encoding most members of the SLAM family are clustered together on mouse chromosome 1 (chr1) and the syntenic region on human chr1 [4,5], referred to here as the *Slamf* gene cluster. *Slamf* genes encode cell surface receptors capable of homophilic and heterophilic interactions which regulate T cell and B cell responses, as well as NK cell, macrophage, dendritic cell, neutrophil and platelet functions. [4,5].

Mouse CD48 (*Slamf2*) is a GPI-anchored glycoprotein expressed by most immune cell types including B and T lymphocytes, NK cells, macrophages and dendritic cells (reviewed in [6]). In mice, CD2 and CD244 (*Slamf4*) are the two known binding partners for CD48. The affinity of CD244 for CD48 is higher than the affinity of CD2 for CD48. CD2 is expressed diffusely by most cells of the immune system, whereas CD244 is expressed on NK cells, intra-epithelial CD8 cells, γδ T cells, myeloid precursors, granulocytes, and monocyte-derived cells. CD48 engagement of CD244 on NK cells can stimulate or inhibit NK cell activity, depending on experimental conditions (reviewed in [7]), while CD48 binding to CD2 on T cell surfaces helps assemble the immunologic synapse and enhances T cell activation [8,9]. CD48 concentrated in T cell lipid rafts behaves as a co-stimulatory molecule when engaged by CD2 [10] or by CD244 [11,12], and crosslinking of CD48 on B cells also has activating effects [13].

CD48-null mice were generated from targeted 129SvJ ES cells injected into C57BL/6 blastocysts and founder animals were backcrossed extensively into the C57BL/6 and BALB/c genetic backgrounds [14,15]. Since these two CD48-deficient strains necessarily retain 129-derived nucleotide sequences flanking the disrupted CD48 gene, they are referred to here as B6.129CD48$^{-/-}$ and Balb.129CD48$^{-/-}$, respectively. Other than slightly increased T cell populations, young B6.129CD48$^{-/-}$ animals appeared healthy [14,15]. Over time, however, naïve B6.129CD48$^{-/-}$ mice developed splenomegaly, hypergammaglobulinemia, autoantibodies against nuclear antigens and proliferative GN [14,15]. Excluding their nephritis, the B6.129CD48$^{-/-}$ lupus-like pattern of autoreactivity mirrored the phenotype of the genetically related CD48-intact B6 congenic strain B6.129-*Sle16* (initially called B6.129chr1b; [16,17]) that possesses a nearly identical span of 129-derived DNA introgressed over the *Slamf* gene cluster on chr1 (Fig. S1). However, the distinct renal phenotypes of the B6.129-*Sle16* strain where some mice acquired mild GN by 12 months of age [17] and the B6.129CD48$^{-/-}$ strain where a majority of animals developed severe GN by 6 months [15], suggest that CD48 ablation had a profound effect on immune activation and

tolerance. Interestingly, Balb.129CD48$^{-/-}$ mice remained healthy with neither systemic nor renal features reminiscent of SLE [14,15]. The differences in these CD48 deficient strains underscore the influence of genetic background even on highly penetrant alleles, and implicate B6-specific genes as essential modifiers of CD48-associated disease.

To further characterize this novel model of lupus nephritis and better understand how CD48 deficiency transforms benign autoreactivity into fatal nephritis, we have studied the natural history of autoimmunity and renal disease in a large cohort of B6.129CD48$^{-/-}$ mice. We demonstrate that CD48-associated GN (CD48GN) is a proliferative GN with low grade proteinuria. It is an immune complex disease with IgG and C3 deposited in a pattern suggestive of ISN/RPS class IV lupus nephritis [18]. In these animals, glomerular inflammation and hypertrophy progress to fibrosis and sclerosis over a period of months, culminating in end stage renal disease before a year of age. Prompted by the contrasting non-autoimmune phenotype of the BALB.129CD48$^{-/-}$ strain, we also evaluated the relative contributions of B6 and BALB/c background genes to the autoimmune phenotype.

2. Material and methods

2.1 Mice

CD48$^{-/-}$ mice of mixed 129 and B6 backgrounds [14] were backcrossed at least 10 generations to BALB/c and B6 mice, respectively, and then independently intercrossed to generate BALB.129CD48$^{-/-}$ and B6.129CD48$^{-/-}$ homozygous strains [15]. B6.129CD48$^{+/-}$ heterozygotes and F1.129CD48$^{-/-}$ animals were generated by crossing B6.129CD48$^{-/-}$ to B6 and to BALB.129CD48$^{-/-}$ strains, respectively. Mice used in this study were housed and cared for in the MGH Thier SPF barrier facility according to IACUC and ALAAC guidelines. MRL/*lpr* (Jackson Laboratory, Bar Harbor, ME) and B6.*FcgR2b*$^{-/-}$ mice (Taconic Farms, Inc., Germantown, NY) were included as disease controls where indicated.

2.2 Histology

Formalin fixed kidneys were stained with H&E and PAS. Blinded scoring of GN severity on a scale from 0 (normal) to 4 (end stage) was based on the presence and severity of mesangial matrix expansion, hypercellularity, capillary wall thickening, capillary loop occlusion, crescentic proliferation, glomerular hypertrophy, hyalinosis and sclerosis. Since the tubulo-interstitial changes lagged behind glomerular pathology, they were not incorporated in the GN scoring system. Morphometric analysis was performed using Openlab imaging processing software (Improvision, Inc., Quincy, MA). Glutaraldehyde fixed kidneys were processed for routine transmission electron microscopy. Immunostaining was performed on acetone fixed renal tissue snap frozen in TissueTek™ OCT compound (Miles, Naperville, IL) and blocked with anti-CD16/CD32 (eBioscience, San Diego, CA). Frozen sections were stained for fluorescence microscopy using FITC-conjugated goat F(ab')2 anti-mouse IgG (DAKO, Denmark) and anti-mouse C3 (ICN/Cappel, Aurora, OH) and for light microscopy using FITC-conjugated lineage specific reagents (anti-CD3, CD4, CD8 (BD pharmingen, San Jose, CA), anti-CD45, B220, CD11b, CD11c, F4/80 and GR-1 (eBioscience, San Diego, CA) and anti-CD68 (Serotec, Inc., Raleigh, NC)) followed by HRP-conjugated F(ab')2 anti-FITC (Roche Molecular Biochemicals, Indianapolis, IN) and VIP substrate (Vector Laboratories, Burlingame, CA). Immunostaining of formalin fixed kidneys was also performed using Borg Decloaker (Biocare Medical, Walnut Creek, CA), DAKO Dual Endogenous Enzyme Block, rat anti-mouse Ki67 (DAKO, Denmark) Biocare Medical Rat on Mouse HRP-Polymer kit, DAB substrate and hematoxylin counterstaining.

2.3 Urine assays

Freshly voided urine samples were tested for hematuria and proteinuria using Hema-Combistix (Siemens Healthcare Diagnostics Inc., Tarrytown, NY). Urine albumin concentrations were measured by ELISA (Bethyl Laboratories Inc., Montgomery, TX) based on manufacturer's guidelines. The albumin concentration of each sample was normalized to urine creatinine that was measured using a colorimetric, picric acid kit (R&D Systems, Minneapolis, MN). Urine neutrophil gelatinase-associated lipocalin (NGAL) levels were measured by ELISA (R&D Systems, Minneapolis, MN) based on manufacturer's guidelines.

2.4 Blood assays

Whole blood was tested for uremia using Azostix (Siemens Healthcare Diagnostics Inc., Tarrytown, NY). Serum levels of total IgG and IgG anti-dsDNA antibodies were tested by ELISA. For total IgG, Immulon 1B microtiter plates (DYNEX, Chantilly, VA) were coated overnight at 4°C with goat anti-mouse IgG (Sigma Chemicals, St. Louis, MO) in PBS. Mouse IgG (Southern Biotech, Birmingham, AL) or serum samples serially diluted in 50% block were applied, followed by alkaline phosphatase-conjugated goat anti-mouse IgG (Southern Biotech, Birmingham, AL) and then p-nitrophenyl phosphate (PNPP) substrate (Sigma Chemicals, St. Louis, MO). For DNA, sera diluted 1:100 were incubated in Immulon 2HB microtiter plates (DYNEX, Chantilly, VA) pre-coated with dsDNA, as described previously [19]. Bound antibodies were detected with phosphatase-conjugated goat anti-mouse IgG and substrate as above. Samples were independently tested at least three times and autoimmune MRL/*lpr* serum was included on each assay plate to normalize between experiments.

2.5 Statistical analysis

Microsoft Office Excel software was used to calculate correlations and perform Student's t-tests as indicated.

3. Results

3.1 B6.129CD48$^{-/-}$ mice have severe immune complex glomerulonephritis

Proliferative GN was previously reported in six of nine B6.129CD48$^{-/-}$ mice aged 6 months [15]. In order to measure the timing of disease onset and the tempo of its progression, we analyzed over 100 B6.129CD48$^{-/-}$ females ranging from 2 to 12 months and compared them to age matched B6 wild type females (B6.WT). This analysis was restricted to non-breeding females in order to exclude confounding effects of hormonal variations and also to simplify the interpretation of glomerular histology which differs at baseline in male and female mice.

To capture disease kinetics, renal histology was scored semiquantitatively for GN severity (0 normal; 1 mild GN; 2 moderate GN; 3 severe GN; 4 ESRD) in H&E and PAS stained kidneys from wild type and CD48-null animals of different ages. Representative images of different grades of CD48GN are shown in Fig. 1 and population data are plotted in Fig. 2. GN was generally not apparent in B6.129CD48$^{-/-}$ mice before 3 to 4 months of age. By 6 months, nearly 50% of the CD48-null females developed nephritis and 75% by 10 months, at which stage over half of them were in renal failure based on BUN measurements (Fig. 2). By contrast, nephritic scores greater than 2 were not seen in B6.WT mice of any age.

Glomerular abnormalities of B6.129CD48$^{-/-}$ mice were initially limited to focal mesangial expansion that could not easily be distinguished from wild type mice (Fig. 1A and B). In 4 to 6 month old animals, disease was marked by glomerular hypertrophy with lobulation and hypercellularity that was both proliferative and inflammatory (Fig. 1C and D). Thickening of the glomerular basement membrane with occlusive endocapillary proliferation and

infiltration also became prominent, but was better appreciated by electron microscopy (see below). CD48GN in 6 to 8 month old females was notable for epithelial cell activation and proliferation in most glomeruli, with fibrocellular crescents seen in many (Fig. 1E and F). Focal karyorrhexis with diffuse inflammation and fibrosis consistent with end stage nephritis was evident in advanced disease (Fig. 1G).

Immunostaining of renal sections was performed to determine whether the GN of the B6.129CD48$^{-/-}$ strain is an immune complex disease as would be required for a model of lupus nephritis. Glomerular IgG and C3 deposition was found in granular patterns in mesangial locations and in peripheral capillary loops (Fig. 3). Transmission electron microscopy better revealed massive mesangial deposits as well as the subendothelial, subepithelial and intramembranous deposits that in combination are essentially diagnostic of lupus in human renal biopsies (Fig. 4). Glomerular inflammation was particularly striking by electron microscopy where mononuclear cells and polymorphic nuclear cells were occluding capillary loops. The electron microscopy was also notable for well preserved podocyte architecture, as opposed to the effacement and fusion of podocyte foot processes generally seen in states of high-grade proteinuria. Taken together, the histological features of GN in B6.129CD48$^{-/-}$ mice is reminiscent of human ISN/RPS class IV lupus nephritis with both acute and chronic components [18].

The urinary findings of mice with CD48GN were similar to those observed in SLE patients with mild but not nephrotic range proteinuria. *In situ* detection of cellular casts in renal histology sections (Fig. 1H) substituted for microscopic examination of a patient's urinary sediment. Testing for urine protein and blood was accomplished using colorimetric dipsticks on random urine samples from B6.129CD48$^{-/-}$ and B6.WT mice of different ages. Hematuria occurred in approximately 30% of B6.129CD48$^{-/-}$ mice whose GN scores exceeded 2 and in 10% of B6.129CD48$^{-/-}$ mice whose renal scores were 2 or less, but never in B6.WT controls (data not shown). Similarly, elevated proteinuria (defined here as a dipstick reading greater than 2+ (>100 mg/dL)) was seen in approximately 30% of mice aged 6-7 months and in 50% of mice aged 8-10 months (Fig. 5A), of whom not all had advanced nephritis. Only 30% of B6.129CD48$^{-/-}$ mice whose GN scores exceeded 2 had proteinuria. For better quantification of proteinuria, albumin concentration in random urine samples was measured by ELISA and normalized to creatinine (Fig. 5B). This analysis demonstrated that with age, B6.129CD48$^{-/-}$ mice developed significant albuminuria compared to wild type controls ($p = 0.004$), but the proteinuria was not nephrotic range and was not associated with hypoalbuminemia (data not shown). This low-grade proteinuria is consistent with the well preserved podocyte foot processes noted by electron microscopy (Fig. 4).

Similar to human SLE, all mice with both hematuria and proteinuria had nephritis with 100% specificity, but a sensitivity of only 7%. In an effort to identify better markers of CD48GN that would substitute for direct histological examination of renal tissue, we borrowed from the human literature [20] and measured levels of neutrophil gelatinase-associated lipocalin (NGAL) as a marker of acute kidney injury in random urine samples from B6.129CD48$^{-/-}$ mice and B6.WT controls. NGAL levels in urine of young, pre-nephritic CD48-null mice were similar to wild type, as expected, but then increased in the older B6.129CD48$^{-/-}$ animals relative to controls ($p < 0.0003$;Fig. 5C). The elevated NGAL was not directly linked to the protein leak of CD48-null mice because B6. *FcgR2b*$^{-/-}$ controls with nephritis and substantially more proteinuria had equivalent levels of urine NGAL (data not shown). Taken together, these data demonstrate that autoimmune renal injury in B6.129CD48$^{-/-}$ mice occurs in absence of high-grade proteinuria.

3.2 CD48GN glomerular hypercellularity is both proliferative and inflammatory, with myeloid predominance

In order to augment our scoring system of renal histology with a quantitative measurement of disease in CD48GN, a morphometric analysis of glomerular size was performed on kidneys from over 100 B6.129CD48$^{-/-}$ and B6.WT animals. The cross sectional area of multiple glomeruli in tissue sections from multiple females were measured digitally and an average glomerular cross sectional area was calculated for each mouse. As expected, glomerular size increased with age in both groups. However, the relative glomerular size as well as the relative growth rates were substantially higher in the B6.129CD48$^{-/-}$ strain compared to B6.WT controls (Fig. 6A). Importantly, these measurements of glomerular size correlated well with the nephritic scores, regardless of genotype (Fig. 6B), thus substantiating and quantifying the hypertrophy noted above in the narrative description of CD48GN.

Since glomerular hypertrophy is due to increased cellularity in addition to mesangial matrix expansion, we next investigated the source of hypercellularity in CD48GN to illuminate mechanisms involved in disease progression. Local proliferation and cellular inflammation could each increase glomerular cellularity in B6.129CD48$^{-/-}$ animals. Since the full extent of cellular proliferation and infiltration would be difficult to appreciate from the rarely noted mitotic figure or migratory WBC seen by routine light microscopy (Fig. 7A), renal sections were stained for the proliferation marker Ki67 and for the pan-leukocyte marker CD45. Glomeruli from B6.129CD48$^{-/-}$ mice had substantially increased nuclear staining for Ki67 relative to age and gender matched controls (Fig. 7B), confirming that CD48GN is proliferative. Whether these dividing cells were resident glomerulocytes or infiltrating leukocytes has not yet been established. Similarly, an analysis of renal cryosections stained for CD45 demonstrated that the total number of WBC (*i.e.* CD45^{+} cells) counted within B6.129CD48$^{-/-}$ glomeruli increased with advancing disease (Fig. 7D). Importantly, not only did inflammatory cell counts per glomerulus increase with disease, but correction for glomerular size verified that WBC counts per glomerular cross sectional area also increased progressively.

Lineage-specific staining of the glomerular infiltrates was subsequently performed on B6.129CD48$^{-/-}$ kidneys in order to determine the cell types involved in pathogenesis. By focusing on animals with relatively early GN, we were able to avoid the florid inflammation associated with end stage nephritis and instead identify the lineages that presumably participate in disease onset. The lymphoid markers used for this survey included CD3, CD4, CD8 and B220 for T cells, T helper cells, T cytotoxic cells and B cells, respectively. The myeloid markers selected were CD11b, F4/80, CD68 (all expressed predominately but not exclusively by monocytes and macrophages), CD11c (dendritic cells) and GR-1 (neutrophils). Immunostaining with this panel of cell lineage markers demonstrated a notable influx of myeloid cells, especially those bearing CD11b, CD68 and CD11c, markers of macrophages and dendritic cells (Fig. 8). There were far fewer GR1^{+} granulocytes and CD4^{+} T cells, although generally more than age matched B6.WT controls. CD8^{+} T cells and B220^{+} B cells were rarely seen in glomeruli of either strain.

In view of the myeloid predominance within the renal infiltrates, B6.129CD48$^{-/-}$ splenic cell populations were re-examined with particular attention to the myeloid lineages that had not been previously characterized. As anticipated from our previous report [15], spleens from the current group of 6 month old non-breeding B6.129CD48$^{-/-}$ females were again significantly larger than age and gender matched B6.WT controls, with a mean weight of 270 mg versus 80 mg, respectively ($p = 0.0002$). Immunostaining of frozen sections with B220 and PNA revealed well preserved white pulp microarchitecture with exuberant germinal center activity in the hyperplastic spleens of naïve B6.129CD48$^{-/-}$ animals (Fig.

S2). Flow cytometry analysis of splenocytes from naïve 6 month old females confirmed previous observations of CD4 T cell expansion and also detected expansion of macrophage and dendritic cell lineages ($p < 0.004$ by Student's t-test for each population). Granulocyte, NK cell, B cell and CD8 T cell population sizes were not different from wild type (Fig. S2).

3.3 CD48-associated autoreactivity is recessive

Contemporaneous with the backcrossing of B6.129CD48$^{-/-}$ mice to the B6 strain, BALB.129CD48$^{-/-}$ animals were also obtained by 10 generations of BALB/c backcrossing from the original B6/129 heterozygous mice [15]. Barring mutations acquired during serial breeding, the B6.129CD48$^{-/-}$ and BALB.129CD48$^{-/-}$ strains are presumed to each have the same CD48-null allele along with flanking DNA of 129 origin carried over from the originally targeted ES cells [14]. Based on microsatellite genotyping, the 129-derived flanking DNA ranges in length from 3 to 14 Mb on the centromeric side of CD48 and 6 to 13 Mb on the telomeric side (Fig. S1).

In contrast to the robust lupus-like phenotype of the B6.129CD48$^{-/-}$ strain, BALB.129CD48$^{-/-}$ mice remained healthy. The BALB.129CD48$^{-/-}$ spleens were of normal size [15] and the mice had normal serum IgG levels (Fig. 9A). They had no autoantibodies against nuclear antigens in general [15] and none against dsDNA in particular (Fig. 9B). Most importantly, BALB.129CD48$^{-/-}$ females remained free of GN for at least 12 months (Fig. 9C). The fact that genetic ablation of CD48 produced lupus-like disease in B6 mice and had no such effect on BALB/c animals suggests that the CD48-associated autoimmune phenotype requires additional genes elsewhere in the B6 genome— distinct from BALB/c alleles— to elicit disease.

In order to test whether the B6 allele(s) putatively important for disease behave in a dominant or recessive manner, F1.129CD48$^{-/-}$ mice were bred from B6.129CD48$^{-/-}$ and BALB.129CD48$^{-/-}$ parental strains. Aging F1.129CD48$^{-/-}$ females were bled for serum at 3 month intervals and sacrificed at 10 months for histology. Like their BALB.129CD48$^{-/-}$ parental strain, F1.129CD48$^{-/-}$ animals appeared to be healthy. They had neither hypergammaglobulinemia nor anti-DNA antibodies by ELISA (Fig. 9A and B). Their renal scores were uniformly non-nephritic and their mean glomerular cross-sectional areas were no different from BALB.129CD48$^{-/-}$ ($p = 0.37$) and were substantially smaller than B6.129CD48$^{-/-}$ samples ($p < 0.0001$;Fig. 9C). The non-autoimmune phenotype of F1.129CD48$^{-/-}$ mice was independent of which parent was B6 and which BALB/c (data not shown).

These F1.129CD48$^{-/-}$ data suggest that the BALB/c genome contains allele(s) with dominant protective effects and/or that disease mediated by this CD48 null allele requires B6 homozygosity at one or more additional loci. To further investigate the question of dominant versus recessive traits in this model system, a group of heterozygous B6.129CD48$^{+/-}$ animals were bred from B6.129CD48$^{-/-}$ and B6.WT parental strains. None of the 13 tested B6.129CD48$^{+/-}$ females had anti-DNA antibodies at 6 months and none had nephritis at 10 months of age (data not shown). This genetic cohort thus demonstrated that a single wild type copy of the B6 strain's CD48 allele was sufficient to restore normal immune function, despite the 129-specific DNA sequences still present on their other copy of chr1.

4. Discussion

We have recently reported that genetic ablation of the SLAM family gene CD48 (*Slamf2*) in 129 ES cells promoted lupus-like disease with nephritis after crossing into C57BL6 but not BALB/C genetic backgrounds [15]. In addition to pursuing the mechanism(s) by which CD48 exerts its protective effect, we have characterized the nephritis in B6.129CD48$^{-/-}$

animals in comparison with human SLE. We now present an extensive analysis of the renal phenotype and natural course of disease in the B6.129CD48$^{-/-}$ mice, demonstrating that this strain constitutes a novel model of lupus nephritis with phenotypes similar to human disease and with features that are both overlapping and distinct from other murine models of SLE.

Referred to as CD48GN, the nephritis of these animals occurs in a setting of systemic autoimmunity notable for excesses in both the adaptive and innate branches of the immune system. Hyperplastic spleens seen in 6 month old B6.129CD48$^{-/-}$ mice had an increased CD4^{+} T cell population [15] as well as increased myeloid cell populations of both macrophage and dendritic cell lineages, suggestive of dysregulated proliferation and/or impaired cell turnover. The enlargement of these splenic populations was associated with spontaneous humoral hyperactivity: T cells displayed activation markers [15], splenic germinal centers were increased in size and number without immunization, and basal levels of circulating immunoglobulin were 2 to 3 times normal. Elevated levels of IgG autoantibodies against nuclear antigens and progressive immune complex GN in these animals are the autoimmune features most evocative of SLE.

CD48GN was seen in a majority of B6.129CD48$^{-/-}$ animals before one year of age and was detectable in some as early as 4 months. Reasons for the variable tempo of disease progression in this and in most other genetic models of lupus are not yet clear, but probably reflect the multigenic multistep nature of disease inherent in human SLE. Regardless, our findings demonstrate that the B6.129CD48$^{-/-}$ autoimmune phenotype unfolds in a reasonably uniform manner. With histopathology more similar to NZB × NZW F1 mice than MRL/*lpr* or BXSB males [21], the early nephritis of CD48GN is characterized by mesangial matrix expansion with glomerular hypertrophy and hypercellularity. The increased glomerular cell counts result from proliferation, as demonstrated by increased Ki67 staining in affected kidneys, and from WBC infiltration. The proliferative and inflammatory responses are presumably elicited by immune complexes that deposit initially in the mesangium and eventually in glomerular capillary loops in subendothelial, sub-epithelial and intramembranous locations. Approximately 30% of animals with CD48GN had hematuria and a majority had low-grade proteinuria. This non-nephrotic range proteinuria is consistent with our ultrastructural observations of intact podocyte foot processes and distinguishes the B6.129CD48$^{-/-}$ strain from many classic [21,22] and from other newly established [23,24] genetic models of lupus nephritis. As expected, urine from nephritic B6.129CD48$^{-/-}$ mice contained elevated levels of the renal injury marker NGAL and animals displayed progressive renal failure within the first year of life.

As the renal profile of B6.129CD48$^{-/-}$ mice models human lupus nephritis fairly well, we surveyed hematopoietic cell lineage-specific markers to determine the composition of glomerular infiltrates and begin to illuminate mechanisms of renal injury. Immunostaining of kidneys in early stages of nephritis revealed that the inflammatory cells in CD48GN glomeruli were predominately myeloid, comprised of both macrophages and dendritic cells. Despite copious glomerular expression of CD11b, CD11c and CD68, F4/80^{+} macrophages were notably absent from the glomeruli and instead accumulated in periglomerular sites. It is possible that the periglomerular subset consisted of resident tissue macrophages and the intraglomerular ones were an inflammatory subset [25,26]. Granulocytes were present in intermediate amounts and CD4^{+} T cells were also seen within many glomeruli, while other lymphocyte subsets were largely lacking. Both light and electron microscopic analyses revealed that many of the glomerular leukocytes were within capillary lumens, possibly reflecting their point of entry into the kidney. Furthermore, the three-fold enlargement of splenic populations expressing macrophage and dendritic cell markers in B6.129CD48$^{-/-}$ mice suggests that CD48 normally regulates these myeloid lineages either directly or indirectly through alterations in T cell function.

The disease of B6.129CD48$^{-/-}$ mice sharply contrasts not only with the healthy phenotype of BALB.129CD48$^{-/-}$ animals but also with their F1.129CD48$^{-/-}$ progeny. Neither the CD48-null BALB homozygotes nor BALB/B6 heterozygotes have any degree of autoimmunity: no immune complex GN nor humoral autoreactivity was seen. These phenotypic differences verify not only that the ablated 129CD48 allele requires the B6 genetic background to evoke autoimmune disease, but that these unidentified B6-specific alleles function in a recessive manner. Xie *et. al.* have shown that interplay between *Sle1b* and *Fas* is responsible for hypersignaling through the PI3K/AKT/mTOR pathway in autoimmune lymphoproliferative disease [27]. Therefore, studies investigating signal transduction via TCR, BCR, and TLRs in B6.129CD48$^{-/-}$ and BALB.129CD48$^{-/-}$ mice may help illuminate the relative contribution of background genes in T cells, B cells, and DCs.

Some of the milder autoimmune features in B6.129CD48$^{-/-}$ mice, such as their anti-nuclear autoantibodies and spontaneously activated CD4^{+} T cells, were also reported in the CD48-intact B6.129-*Sle16* strain whose CD48 gene and flanking loci on a 24 Mb segment of chr1 had been replaced with 129-specific sequences (Fig. S1) [16]. It is tempting to infer that those autoimmune phenotypes shared by the B6.129CD48$^{-/-}$ and B6.129-*Sle16* strains are driven by similar epistatic interactions between 129-derived allele(s) on chr1 and B6-specific sequences elsewhere in the genome [16], and are independent of CD48 itself.

Two haplotypes have been identified for this gene-dense region of chr1. “Haplotype 1” is shared by a majority of inbred strains including 129, NZB, NZW and BALB/c, whereas B6 is one of the few strains with “haplotype 2” [2]. Like the B6.129-*Sle16* mice with haplotype 1 of 129 origin, congenic strains B6. *Nba2* -A'B [28] and B6.*Sle1b* [29] carry overlapping NZB and NZW derived haplotype 1 sequences, respectively, and they also display a “benign” autoimmune phenotype (Fig. S1). Experiments on B6.*Sle1b* mice have implicated *Slamf6* as a candidate within this region that confers the autoreactivity [30] and linkage analysis of B6 × 129 mixed progeny have mapped B6 lupus susceptibility loci to chromosomes 13 and 3 [31].

Fatal nephritis is the salient lupus phenotype that distinguishes B6.129CD48$^{-/-}$ mice from the aforementioned CD48-intact strains. This distinction suggests that CD48 expression protects the lupus-prone congenics from disease, whereas CD48 deficiency in B6.129CD48$^{-/-}$ animals transforms a “pre-lupus” phenotype into fulminant lupus nephritis. The broad expression of CD48 on a variety of hematopoietic cell types suggests that CD48 may regulate immune responses in a number of ways. Studies using CD48 deficient mice have revealed roles for CD48 in controlling T cell and macrophage function. Defects in the T cell compartment have been revealed by *in vitro* experiments demonstrating poor activation of T cells from B6.129CD48$^{-/-}$ [14] and from BALB.129CD48$^{-/-}$ mice [32]. *In vivo* studies demonstrated impaired T cell tolerance induction in BALB.129CD48$^{-/-}$ animals as well as poor IgG responses to T-dependent but not T-independent antigens [15]. LPS triggered a lesser response in CD48-deficient macrophages compared to wild type, and antigen-pulsed CD48$^{-/-}$ macrophages stimulated wild type antigen specific T cells poorly when compared to wild type APCs [32]. The healthy phenotype of BALB.129CD48$^{-/-}$ mice suggests that these abnormalities have limited impact in naïve mice from an otherwise non-autoimmune strain, while dysfunctional T cells and macrophages could disrupt tolerogenic safeguards in B6.129CD48$^{-/-}$ animals in ways that intensify the autoreactivity driven by 129 allele(s) on chr1.

One can look to the CD48 binding partners CD2 and CD244 to help understand mechanism of disease, particularly since expression of each is upregulated in CD48-null mice [14,15]. The absence of nephritis in B6.CD2$^{-/-}$ mice whose targeted gene is on chr3 [33] and in B6.CD244$^{-/-}$ mice whose targeted gene resides in the *Slamf* gene cluster but was generated

with B6 rather than 129 ES cells [34] might suggest that there is enough functional redundancy between CD48:CD2 and CD48:CD244 interactions that only loss of CD48 itself yields an overt phenotype. It may also indicate that CD48 has another receptor or ligand to be identified. Most likely, however, these “counter-receptor” deficient strains are B6 congenics that each have the B6-specific alleles (haplotype 2) of the *Slamf* gene cluster rather than the 129-derived haplotype 1, and hence lack one of the genetic components critical to this model of lupus nephritis.

5. Conclusions

The SLAM family member CD48 is a cell surface molecule that modulates immune tolerance. The grave consequences of CD48 deficiency in the B6 genetic background include progressive autoimmune disease with fatal nephritis. The GN of B6.129CD48$^{-/-}$ mice is a diffuse, proliferative immune complex disease that models human SLE nephritis in a number of ways, causing hematuria, low-grade proteinuria and renal failure. Both lymphoid and myeloid cell dysfunction appear to be present in CD48GN. In contrast to B6, CD48-deficiency in the BALB/c genetic background generates no autoreactivity. B6 × BALB/c F1.129CD48$^{-/-}$ mice are likewise spared, as are B6.129CD48$^{+/-}$ heterozygotes. In light of growing evidence that the 129 haplotype of the *Slamf* gene cluster drives benign autoimmunity in B6 mice, our findings indicate that three genetic features (a) homozygous CD48 deficiency, (b) 129 genomic DNA abutting the disrupted CD48 allele, and (c) specific but yet unknown loci from the B6 genome conspire to elicit disease in this novel model of lupus nephritis.

Supplementary Material

Refer to Web version on PubMed Central for supplementary material.

Acknowledgments

We thank Tricia Della Pelle for technical support and Harald Jueppner and Adam Lacy-Hulbert for critical reading of the manuscript. This work was supported by awards from the Lupus Research Institute and NIH R01DK079989 to EP and NIH P01AI-065687 to AHS and YEL.

References

1. Engel P, Eck MJ, Terhorst C. The SAP and SLAM families in immune responses and X-linked lymphoproliferative disease. Nat Rev Immunol. 2003; 3:813–21. [PubMed: 14523387]
2. Wandstrat AE, Nguyen C, Limaye N, Chan AY, Subramanian S, Tian XH, Yim YS, Pertsemlidis A, Garner HR Jr, Morel L, Wakeland EK. Association of extensive polymorphisms in the SLAM/CD2 gene cluster with murine lupus. Immunity. 2004; 21:769–80. [PubMed: 15589166]
3. Cunninghame Graham DS, Vyse TJ, Fortin PR, Montpetit A, Cai YC, Lim S, McKenzie T, Farwell L, Rhodes B, Chad L, Hudson TJ, Sharpe A, Terhorst C, Greenwood CM, Wither J, Rioux JD. Association of LY9 in UK and Canadian SLE families. Genes Immun. 2008; 9:93–102. [PubMed: 18216865]
4. Boles KS, Stepp SE, Bennett M, Kumar V, Mathew PA. 2B4 (CD244) and CS1: novel members of the CD2 subset of the immunoglobulin superfamily molecules expressed on natural killer cells and other leukocytes. Immunol Rev. 2001; 181:234–49. [PubMed: 11513145]
5. Tangye SG, Phillips JH, Lanier LL. The CD2-subset of the Ig superfamily of cell surface molecules: receptor-ligand pairs expressed by NK cells and other immune cells. Semin Immunol. 2000; 12:149–57. [PubMed: 10764623]
6. Elishmereni M, Levi-Schaffer F. CD48: A co-stimulatory receptor of immunity. Int J Biochem Cell Biol. 43:25–8. [PubMed: 20833258]

7. Bhat R, Eissmann P, Endt J, Hoffmann S, Watzl C. Fine-tuning of immune responses by SLAM-related receptors. J Leukoc Biol. 2006; 79:417–24. [PubMed: 16365151]
8. Wild MK, Cambiaggi A, Brown MH, Davies EA, Ohno H, Saito T, van der Merwe PA. Dependence of T cell antigen recognition on the dimensions of an accessory receptor-ligand complex. J Exp Med. 1999; 190:31–41. [PubMed: 10429668]
9. Latchman Y, Reiser H. Enhanced murine CD4+ T cell responses induced by the CD2 ligand CD48. Eur J Immunol. 1998; 28:4325–31. [PubMed: 9862369]
10. Moran M, Miceli MC. Engagement of GPI-linked CD48 contributes to TCR signals and cytoskeletal reorganization: a role for lipid rafts in T cell activation. Immunity. 1998; 9:787–96. [PubMed: 9881969]
11. Assarsson E, Kambayashi T, Schatzle JD, Cramer SO, von Bonin A, Jensen PE, Ljunggren HG, Chambers BJ. NK cells stimulate proliferation of T and NK cells through 2B4/CD48 interactions. J Immunol. 2004; 173:174–80. [PubMed: 15210772]
12. Kambayashi T, Assarsson E, Chambers BJ, Ljunggren HG. Cutting edge: Regulation of CD8(+) T cell proliferation by 2B4/CD48 interactions. J Immunol. 2001; 167:6706–10. [PubMed: 11739483]
13. Gao N, Jennings P, Yuan D. Requirements for the natural killer cell-mediated induction of IgG1 and IgG2a expression in B lymphocytes. Int Immunol. 2008; 20:645–57. [PubMed: 18339657]
14. Gonzalez-Cabrero J, Wise CJ, Latchman Y, Freeman GJ, Sharpe AH, Reiser H. CD48-deficient mice have a pronounced defect in CD4(+) T cell activation. Proc Natl Acad Sci U S A. 1999; 96:1019–23. [PubMed: 9927686]
15. Keszei M, Latchman YE, Vanguri VK, Brown DR, Detre C, Morra M, Arancibia CV, Paul E, Calpe S, Castro W, Wang N, Terhorst C, Sharpe AH. Auto-antibody production and glomerulonephritis in congenic Slamf1-/- and Slamf2-/- [B6.129] but not in Slamf1-/- and Slamf2-/- [BALB/c.129] mice. Int Immunol. 2011; 23:149–58. [PubMed: 21278219]
16. Carlucci F, Cortes-Hernandez J, Fossati-Jimack L, Bygrave AE, Walport MJ, Vyse TJ, Cook HT, Botto M. Genetic dissection of spontaneous autoimmunity driven by 129-derived chromosome 1 Loci when expressed on C57BL/6 mice. J Immunol. 2007; 178:2352–60. [PubMed: 17277141]
17. Carlucci F, Fossati-Jimack L, Dumitriu IE, Heidari Y, Walport MJ, Szajna M, Baruah P, Garden OA, Cook HT, Botto M. Identification and characterization of a lupus suppressor 129 locus on chromosome 3. J Immunol. 2010; 184:6256–65. [PubMed: 20435933]
18. Weening JJ, D'Agati VD, Schwartz MM, Seshan SV, Alpers CE, Appel GB, Balow JE, Bruijn JA, Cook T, Ferrario F, Fogo AB, Ginzler EM, Hebert L, Hill G, Hill P, Jennette JC, Kong NC, Lesavre P, Lockshin M, Looi LM, Makino H, Moura LA, Nagata M. The classification of glomerulonephritis in systemic lupus erythematosus revisited. Kidney Int. 2004; 65:521–30. [PubMed: 14717922]
19. Paul E, Pozdnyakova OO, Mitchell E, Carroll MC. Anti-DNA autoreactivity in C4-deficient mice. Eur J Immunol. 2002; 32:2672–9. [PubMed: 12207352]
20. Brunner HI, Mueller M, Rutherford C, Passo MH, Witte D, Grom A, Mishra J, Devarajan P. Urinary neutrophil gelatinase-associated lipocalin as a biomarker of nephritis in childhood-onset systemic lupus erythematosus. Arthritis Rheum. 2006; 54:2577–84. [PubMed: 16868980]
21. Andrews BS, Eisenberg RA, Theofilopoulos AN, Izui S, Wilson CB, McConahey PJ, Murphy ED, Roths JB, Dixon FJ. Spontaneous murine lupus-like syndromes. Clinical and immunopathological manifestations in several strains. J Exp Med. 1978; 148:1198–215. [PubMed: 309911]
22. Theofilopoulos AN, Dixon FJ. Murine models of systemic lupus erythematosus. Adv Immunol. 1985; 37:269–390. [PubMed: 3890479]
23. Bolland S, Ravetch JV. Spontaneous autoimmune disease in Fc(gamma)RIIB-deficient mice results from strain-specific epistasis. Immunity. 2000; 13:277–85. [PubMed: 10981970]
24. Morel L, Croker BP, Blenman KR, Mohan C, Huang G, Gilkeson G, Wakeland EK. Genetic reconstitution of systemic lupus erythematosus immunopathology with polycongenic murine strains. Proc Natl Acad Sci U S A. 2000; 97:6670–5. [PubMed: 10841565]
25. Masaki T, Chow F, Nikolic-Paterson DJ, Atkins RC, Tesch GH. Heterogeneity of antigen expression explains controversy over glomerular macrophage accumulation in mouse glomerulonephritis. Nephrol Dial Transplant. 2003; 18:178–81. [PubMed: 12480978]

26. Li L, Huang L, Sung SS, Vergis AL, Rosin DL, Rose CE Jr, Lobo PI, Okusa MD. The chemokine receptors CCR2 and CX3CR1 mediate monocyte/macrophage trafficking in kidney ischemia-reperfusion injury. Kidney Int. 2008; 74:1526–37. [PubMed: 18843253]
27. Xie C, Patel R, Wu T, Zhu J, Henry T, Bhaskarabhatla M, Samudrala R, Tus K, Gong Y, Zhou H, Wakeland EK, Zhou XJ, Mohan C. PI3K/AKT/mTOR hypersignaling in autoimmune lymphoproliferative disease engendered by the epistatic interplay of Sle1b and FASlpr. Int Immunol. 2007; 19:509–22. [PubMed: 17369192]
28. Jorgensen TN, Alfaro J, Enriquez HL, Jiang C, Loo WM, Atencio S, Bupp MR, Mailloux CM, Metzger T, Flannery S, Rozzo SJ, Kotzin BL, Rosemblatt M, Bono MR, Erickson LD. Development of murine lupus involves the combined genetic contribution of the SLAM and FcgammaR intervals within the Nba2 autoimmune susceptibility locus. J Immunol. 2010; 184:775–86. [PubMed: 20018631]
29. Morel L, Blenman KR, Croker BP, Wakeland EK. The major murine systemic lupus erythematosus susceptibility locus, Sle1, is a cluster of functionally related genes. Proc Natl Acad Sci U S A. 2001; 98:1787–92. [PubMed: 11172029]
30. Kumar KR, Li L, Yan M, Bhaskarabhatla M, Mobley AB, Nguyen C, Mooney JM, Schatzle JD, Wakeland EK, Mohan C. Regulation of B cell tolerance by the lupus susceptibility gene Ly108. Science. 2006; 312:1665–9. [PubMed: 16778059]
31. Heidari Y, Bygrave AE, Rigby RJ, Rose KL, Walport MJ, Cook HT, Vyse TJ, Botto M. Identification of chromosome intervals from 129 and C57BL/6 mouse strains linked to the development of systemic lupus erythematosus. Genes Immun. 2006; 7:592–9. [PubMed: 16943797]
32. Abadia-Molina AC, Ji H, Faubion WA, Julien A, Latchman Y, Yagita H, Sharpe A, Bhan AK, Terhorst C. CD48 controls T-cell and antigen-presenting cell functions in experimental colitis. Gastroenterology. 2006; 130:424–34. [PubMed: 16472597]
33. Killeen N, Stuart SG, Littman DR. Development and function of T cells in mice with a disrupted CD2 gene. Embo J. 1992; 11:4329–36. [PubMed: 1358605]
34. Lee KM, McNerney ME, Stepp SE, Mathew PA, Schatzle JD, Bennett M, Kumar V. 2B4 acts as a non-major histocompatibility complex binding inhibitory receptor on mouse natural killer cells. J Exp Med. 2004; 199:1245–54. [PubMed: 15123744]

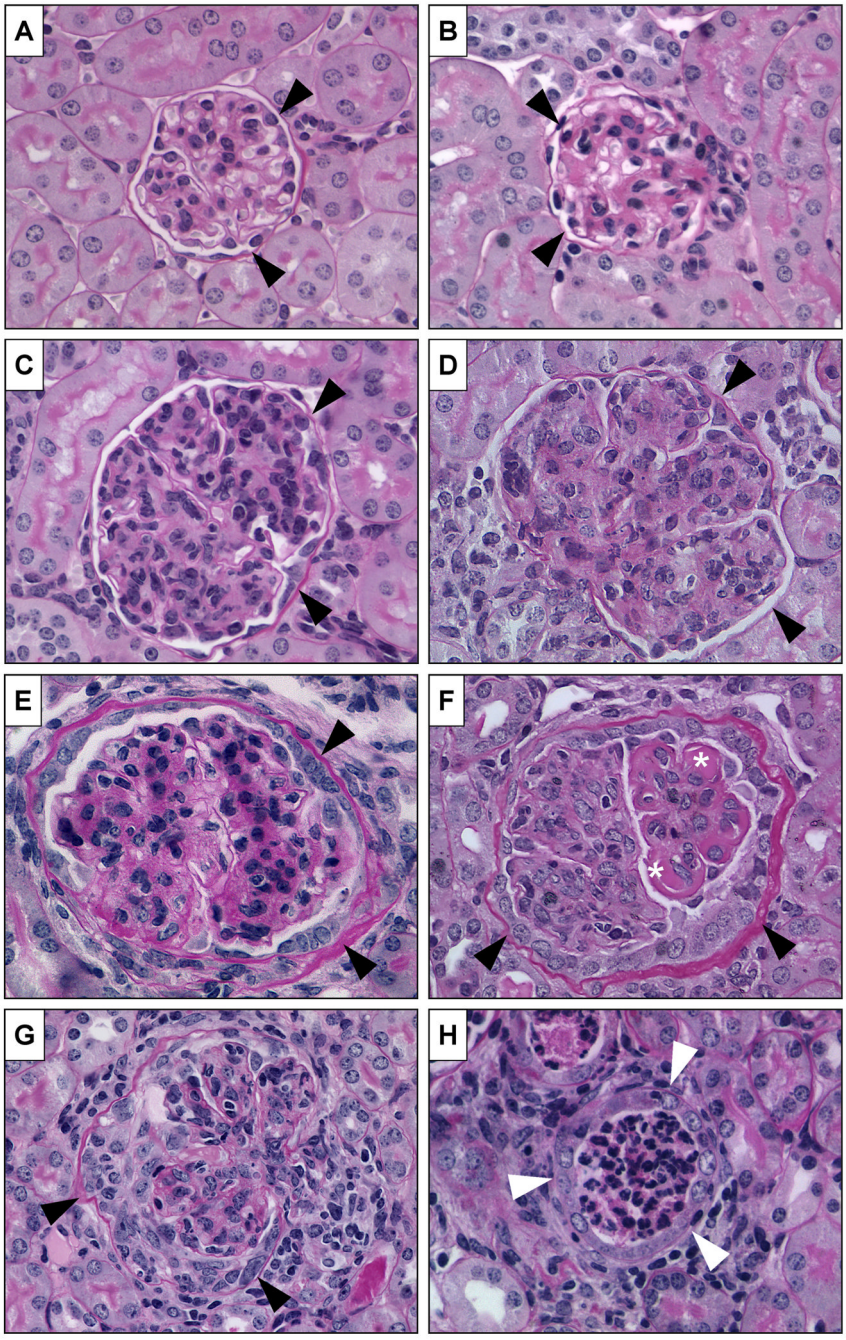

Figure 1. CD48GN is proliferative and crescentic

Representative PAS stained glomeruli from kidneys of B6.WT (A) and B6.129CD48$^{-/-}$ females (B-G) show the pathologic features characteristic of GD48GN at 400× magnification. Mesangial accentuation was barely discernable in young B6.129CD48$^{-/-}$ mice whose glomerular architecture appeared relatively normal (B). Progression to glomerular hypertrophy, hypercellularity and lobulation (C and D) was seen diffusely in most B6.129CD48$^{-/-}$ animals by 4-5 months and never in wild type controls. The loss of open capillary loops at this stage was presumably mirrored by a gradual impairment of renal function. Normally flattened against Bowman's capsule (marked by black arrowheads), parietal podocytes transitioned into a cuboidal epithelium and proliferated to form

multilayered cellular crescents (E and F). Some animals also acquired pseudothrombi (white asterisks) that are indicative of cryoglobulinemia in human SLE. Proliferation and infiltration eventually obliterated the glomerular tuft (G). A WBC cast caught within a B6.129CD48$^{-/-}$ tubule demarcated by white arrowheads is shown in panel H.

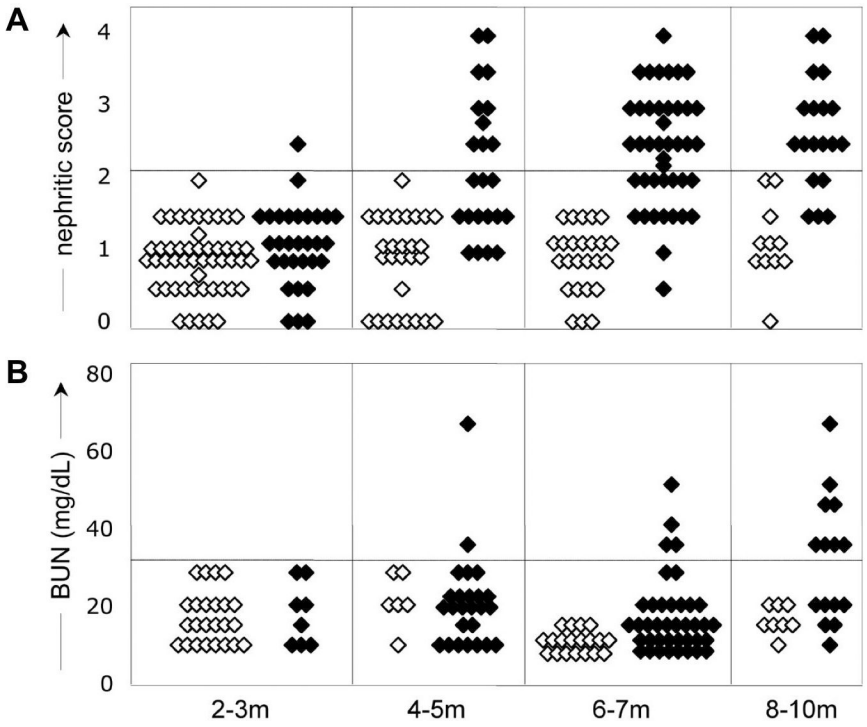

Figure 2. Most B6.129CD48$^{-/-}$ mice acquire GN by 6 months and renal failure by 12 months

Panel A: PAS stained kidney sections from mice of different ages were scored for glomerular abnormalities on a scale from 0 to 4 (11-50 animals per group). B6.WT females (open symbols) developed little pathology other than mild mesangial expansion, whereas progressive nephritis became apparent in half of B6.129CD48$^{-/-}$ mice (filled symbols) by 6 months of age and 75% by 10 months. The nephritic scores were significantly higher in B6.129CD48$^{-/-}$ versus B6.WT kidneys ($p < 3\times10^{-6}$ by Student's t-test) in each of the 3 older age groups.

Panel B: Blood urea nitrogen (BUN) was measured by colorimetric dipstick in whole blood samples from females of different ages (8-39 animals per group). Only B6.129CD48$^{-/-}$ mice (filled symbols) developed uremia, generally at advanced age with advanced disease. BUN measurements were significantly different between B6.129CD48$^{-/-}$ and B6.WT (open symbols) mice in both the 6-7 and the 8-10 month age groups ($p < 0.003$ by Student's t-test).

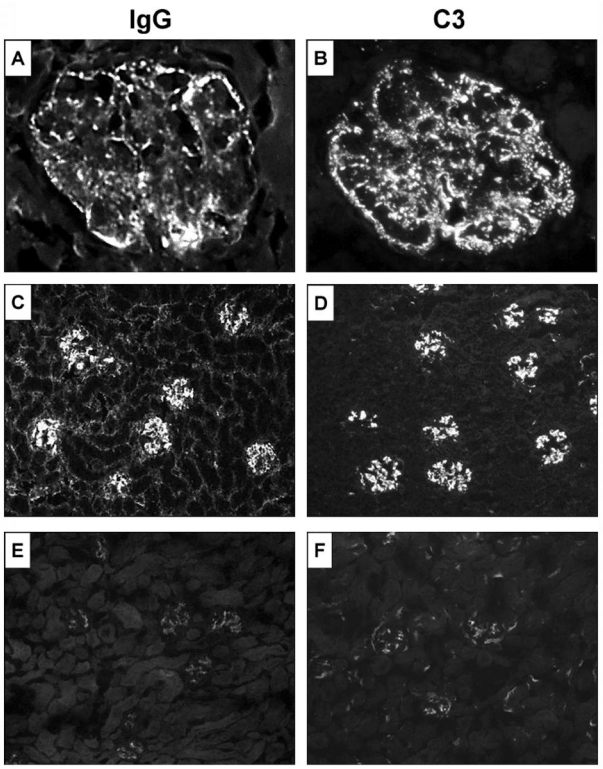

Figure 3. CD48GN is an immune complex disease

Frozen kidney sections from 6 month old B6.129CD48$^{-/-}$ and B6.WT mice were stained for immunoglobulin IgG and for complement C3, as labeled. High power immunofluorescence images of CD48-null glomeruli (A and B) show immune complexes in granular patterns along the capillary walls. Mesangial deposits are also appreciated in the low power images of B6.129CD48$^{-/-}$ renal cortex (C and D) but not in age and gender matched B6.WT controls (E and F). High and low power magnifications were 600 and 400×, respectively.

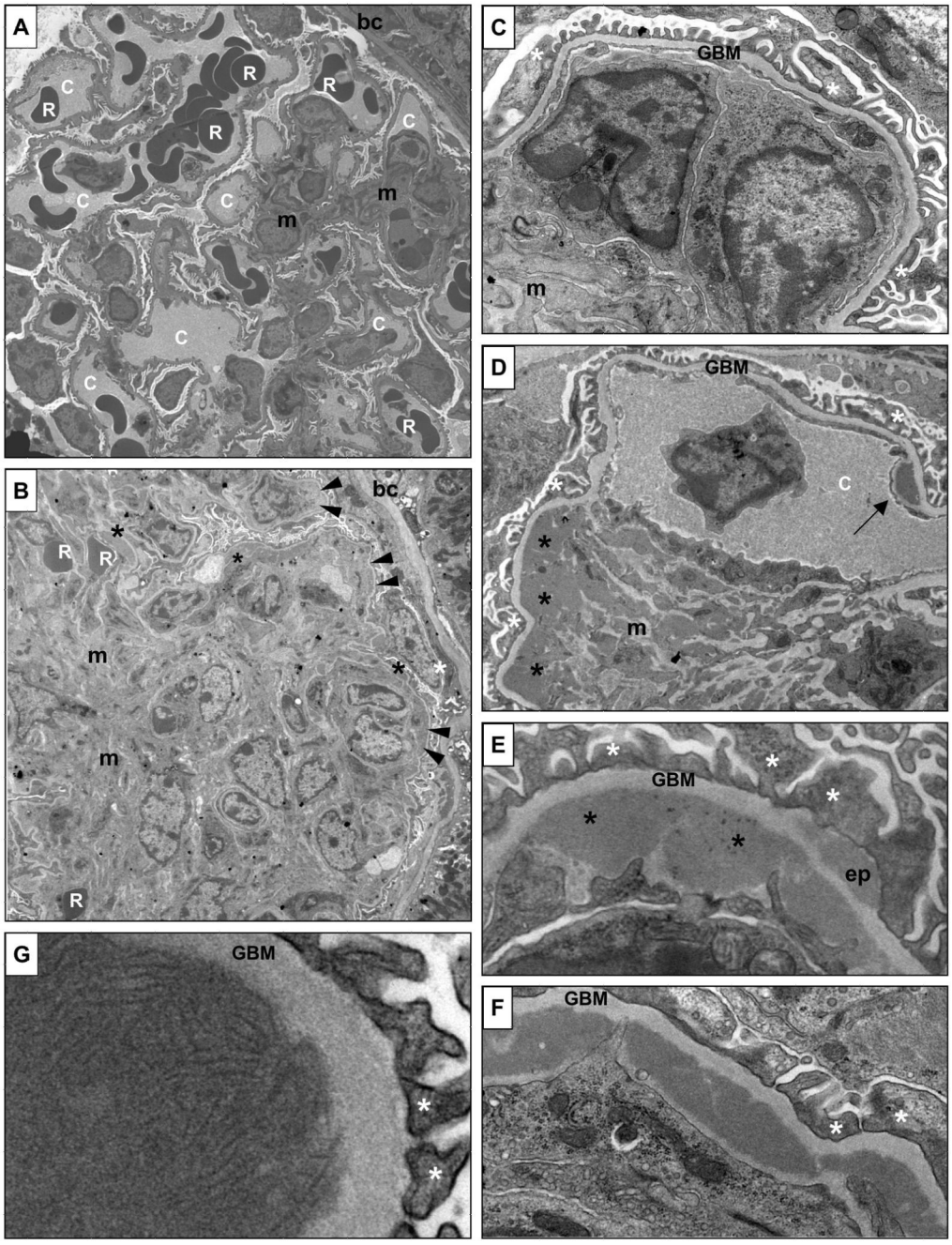

Figure 4. Glomerular deposits in CD48GN are typical of lupus nephritis

Low power electron microscopic views of normal and nephritic glomeruli are shown in panels A and B, respectively, with Bowman's capsule labeled “bc”; capillaries “c”; red blood cells “R”; mesangium “m”. Patent capillary loops and plentiful erythrocytes are easily seen in the normal glomerulus of panel A but are hardly discernible in the nephritic glomerulus of panel B. Instead, capillaries marked by black arrowheads are nearly obliterated by swollen endothelium and occlusive intraluminal inflammatory cells as well as expanded mesangium. Electron dense deposits (black asterisks) are difficult to see at this magnification. Higher power views of capillary loops from nephritic mice are shown in panels C and D. The capillary in panel C is occluded by two mononuclear cells surrounded by a thin rim of

endothelial cell cytoplasm lining the glomerular basement membrane (GBM). The podocytes encasing this capillary loop (white asterisks) have well preserved foot processes without the fusion and effacement that usually accompanies high-grade proteinuria. The patent capillary loop shown in panel D is notable for an isolated subendothelial deposit on the right (black arrow) as well as mesangial and paramesangial deposits (black asterisks) forming a layered pattern that implicates serial waves of immune insult. This loop's podocyte architecture is also reasonably well preserved, as are the foot processes shown at still higher magnification in panels E, F and G (white asterisks). High power views of electron dense subendothelial (black asterisks) and subepithelial (“ep”) deposits are displayed in panel E, as well as intramembranous deposits in panel F. Panel G shows the fibrillary microarchitecture of a stereotypical “fingerprint” deposit sometimes seen in human lupus biopsies. Approximate magnifications: A and B 2000×; C and D 9000×; E and F 25000×; G 40000×. Abbreviations and markings: bc= Bowman's capsule; c= capillary lumen; ep= subepithelial deposit; GBM= glomerular basement membrane; R= red blood cell; white asterisk= podocytes; black asterisks= electron dense deposits; black arrowheads= capillary loops; black arrow= subendothelial deposit.

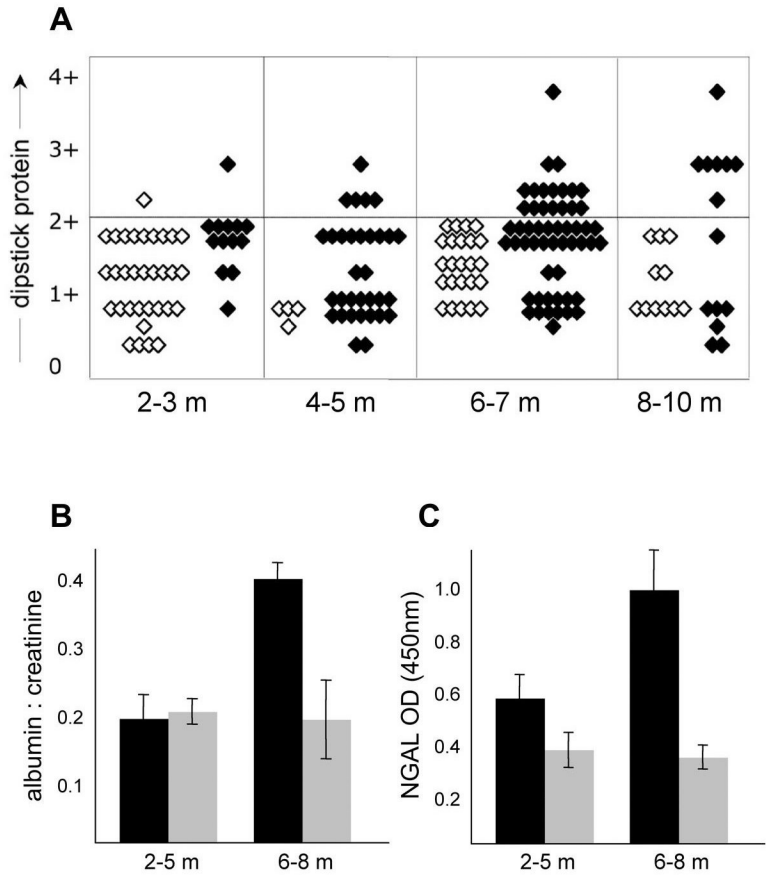

Figure 5. CD48GN is associated with low-grade proteinuria

Panel A: Protein was measured by colorimetric dipstick in random urine samples from female mice of different ages. Many B6.129CD48$^{-/-}$ mice (filled symbols) developed proteinuria with age, relative to B6.WT mice (open symbols) whose urine rarely dipped greater than 2+ (100 mg/dL).

Panel B: Albumin and creatinine concentrations in random urine samples were measured by ELISA and picric acid assay, respectively. B6.129CD48$^{-/-}$ females (black bars) had normal urine albumin levels until 5 months when proteinuric B6.*FcgR2b*$^{-/-}$ controls had 8-fold higher albumin to creatinine ratios (data not shown). Aging B6.129CD48$^{-/-}$ mice had increased albuminuria that was not nephrotic range but was nonetheless significantly higher than B6.WT controls (gray bars; p=0.004). Error bars are standard error of the mean for 13-30 females per group.

Panel C: An ELISA was used to measure urine NGAL as a surrogate marker of renal injury. At younger ages, samples from B6.129CD48$^{-/-}$ (black bars) had slightly higher levels of urine NGAL than wild type controls (gray bars; p=0.08). Subsequently, urine NGAL levels rose significantly with age in CD48-null but not in wild type animals (p = 0.0003), presumably reflecting progression of their glomerular disease. Error bars are standard error of the mean for 19-51 females per group.

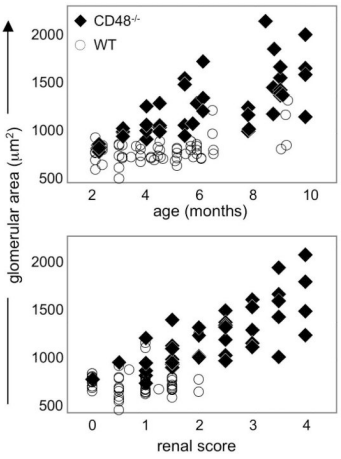

Figure 6. Glomeruli hypertrophy in CD48GN

Glomerular cross sectional areas were measured in kidney sections from B6.129CD48$^{-/-}$ and wild type mice of different ages at different stages of disease (N=61 and 43, respectively). Progressive glomerular hypertrophy is apparent when the average glomerular cross sectional area from individual animals is plotted against age (upper plot), where each symbol represents the mean of 10 to 20 glomeruli per mouse. Filled diamonds denote B6.129CD48$^{-/-}$ mice whose glomeruli grew faster and became significantly larger than B6.WT glomeruli (open symbols), with slopes of 86 and 33 μm^2/month, respectively ($p < 0.001$). Importantly, these measurements of glomerular size correlated well with the nephritic scores, regardless of age and genotype (lower plot; $r = 0.78$; $p < 0.001$).

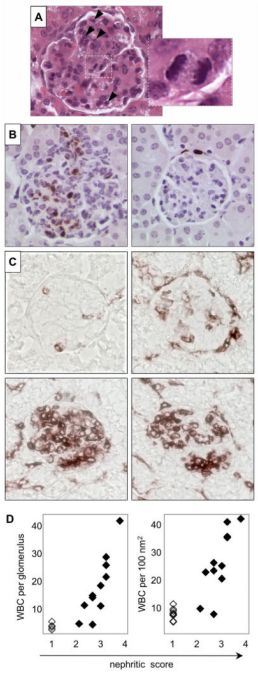

Figure 7. Glomerular hypercellularity is both inflammatory and proliferative

Panel A: H&E staining reveals a mitotic figure in the middle of this mildly nephritic CD48$^{-/-}$ glomerulus with a chromatin configuration consistent with anaphase (inset). Black arrowheads mark some of the leukocytes infiltrated into the glomerulus. **Panel B:** Immunostaining for Ki67 reveals abundant proliferation in B6.129CD48$^{-/-}$ glomeruli (left) but very little in B6.WT animals (right). In these images counterstained with hematoxylin, Ki67 positive nuclei stained brown. **Panel C:** Frozen kidney sections were stained for the pan-leukocyte marker CD45 in order to identify inflammatory cells. Starting in the upper left and moving clockwise, four photographs of B6.129CD48$^{-/-}$ glomeruli show the infiltrates that accompany relatively early disease progression, before crescentic and sclerotic changes are seen. Extra-glomerular WBC are also visible in these images. Quantification of this progressive inflammation is depicted in **panel D** where the number of CD45^{+} cells per glomerulus (left graph) and the number of CD45^{+} cells per glomerular cross sectioned area (right graph) are plotted against nephritic scores. Each symbol represents the mean cell count per mouse. Mean B6.129CD48$^{-/-}$ and wild type counts are indicated by filled and open symbols, respectively. All GN scores of 1 are from B6.WT mice whereas all higher scores are from B6.129CD48$^{-/-}$ animals.

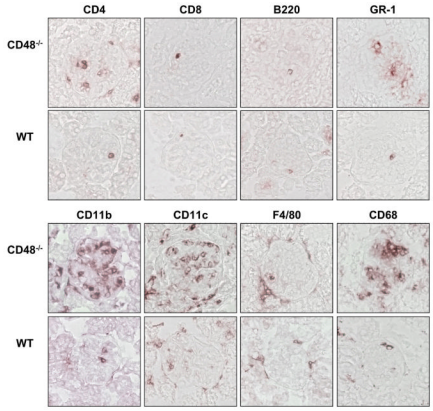

Figure 8. Myeloid cells infiltrates predominate in CD48GN

Kidneys from 6 month old B6.129CD48$^{-/-}$ females with mild to moderate GN were stained for lineage-specific markers to identify the infiltrating cell types. Markers for T and B lymphocytes and for granulocytes are displayed in the upper panels alongside wild type controls, whereas markers for monocytes/ macrophages and dendritic cells are in the lower panels. In the CD4, GR-1, CD11b, CD11c and CD68 immunostainings there are multiple if not numerous lineage-positive cells stained brown in the B6.129CD48$^{-/-}$ glomeruli, and these particular images are representative of the whole kidney section. In contrast, the displayed "single cell glomeruli" (*e.g.* CD8, B220 and F4/80) are not representative images but instead were selected to demonstrate effective immunostaining while also indicating that these cell types are distributed quite sparsely through the renal cortex and that many glomeruli are in fact devoid of these lineages. CD3 staining mirrors CD4 quite closely and is therefore not shown.

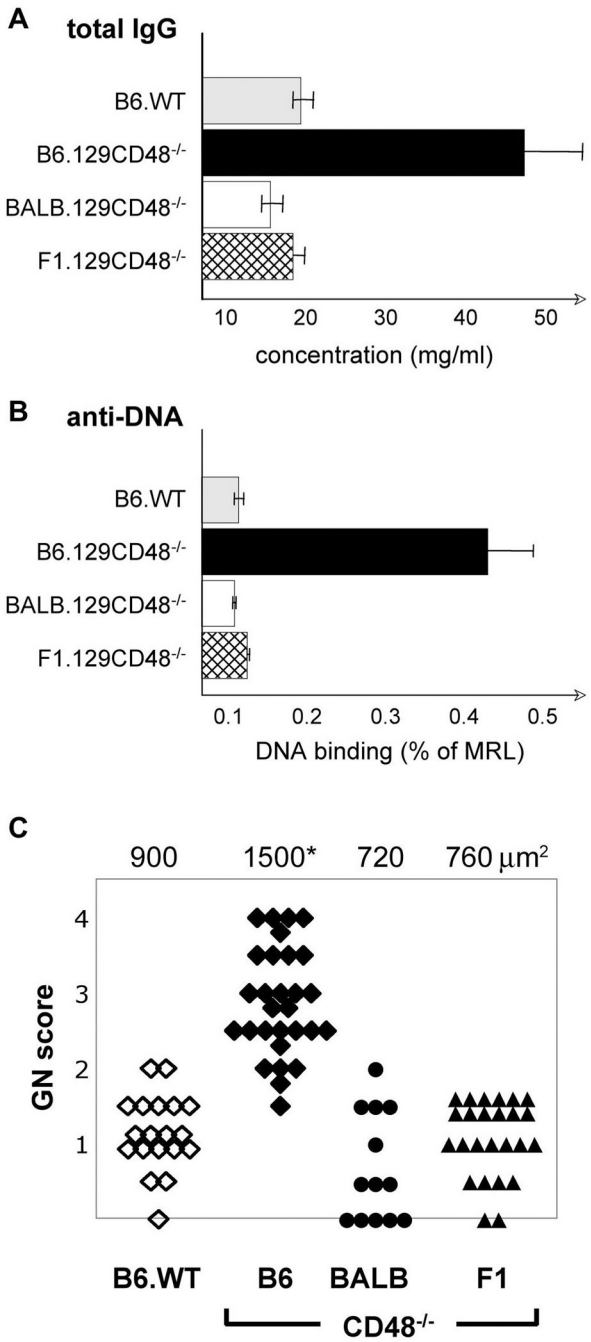

Figure 9. CD48-associated autoimmunity depends on recessive B6 specific alleles

Panels A and B show the mean total IgG concentrations and the mean IgG anti-DNA activity, respectively, in serum samples from B6.WT (gray), B6.129CD48$^{-/-}$ (black), BALB.129CD48$^{-/-}$ (white) and F1.129CD48$^{-/-}$ (hatched) females at 6 months of age. Each ELISA group had 6-14 mice; error bars reflect standard error of the mean. B6.129CD48$^{-/-}$ mice had significantly more circulating IgG and more IgG anti-DNA activity than each of the other groups ($p < 0.003$ in all cases by Student's t-test).

Panel C: PAS stained kidney sections from 8 to 10 month old CD48$^{-/-}$ female mice of different genetic backgrounds were scored for GN. Only B6.129CD48$^{-/-}$ mice had disease. Glomerular histology of age matched Balb.129CD48$^{-/-}$ and F1.129CD48$^{-/-}$ females were no

different from B6.WT controls. The mean glomerular cross-sectional area for each genotype is indicated above the plot, with only B6.129CD48$^{-/-}$ kidneys showing significant glomerular hypertrophy ($p < 0.0001$).